# Effect of stacking sequence of fibre metal laminates with carbon fibre reinforced composites on mechanical attributes: Numerical simulations and experimental validation

N. Rajesh Jesudoss Hynes [a], N.J. Vignesh [a,**], J.T. Winowlin Jappes [b], P. Shenbaga Velu [c], Claudia Barile [d], Muhammad Asad Ali [e,***], Muhammad Umar Farooq [f,****], Catalin I. Pruncu [g,h,*]

[a] Department of Mechanical Engineering, Mepco Schlenk Engineering College, Sivakasi, India
[b] Department of Mechanical Engineering, Kalasalingam University, Krishnankovil, India
[c] Department of Mechanical Engineering, PSR Engineering College, Sivakasi, India
[d] Dipartimento di Meccanica, Matematica e Management, Politecnico di Bari, Viale Japigia 182, 70126, Bari, Italy
[e] Department of Industrial and Manufacturing Engineering, University of Engineering and Technology, Lahore, 54890, Pakistan
[f] School of Mechanical Engineering, The University of Leeds, LS2 9JT Leeds, UK
[g] Department of Mechanical Engineering, Imperial College London, London, SW7 2AZ, UK
[h] Design, Manufacturing & Engineering Management, University of Strathclyde, Glasgow, G1 1XJ, Scotland, UK

## ARTICLE INFO

## ABSTRACT

Fibre Metal Laminates are structures used primarily in aerospace applications because of their principal advantages such as high strength, lower density, and impact resistance. In the present work, a systematic assessment has been made to evaluate two different stacking sequences of FMLs (Type – I (AA 6061/Carbon Fibre/AA 6061/Carbon Fibre/AA 6061), and Type – II (Carbon Fibre/AA 6061/Carbon Fibre/AA 6061/Carbon Fibre)) against a pure carbon composite (Type - III) as baseline for improvement. The investigations are made for enhanced impact resistance, improved tensile strength, increased flexural capability, microstructural evolution, and surface composition. Mechanical-based testing resulted that Type – I shows significant performance followed by Type – II. The maximum values of tensile strength, impact test, and ultimate load bearing capacity of during flexural test were around 192.92 MPa, 9.3 J, and 155 N, respectively. Correlations of experimental results were drawn against numerical simulation to validate the tensile and flexural results. Microstructural evolution indicated good bonding capability of Type – I FML with the carbon fibre. EDX analysis was carried out analyse surface chemistry. Selected Fibre Metal Laminate sequence can help in improving aeronautical industry's structural applications because of good ductile properties together with fatigue strength and impact resistance.

## 1. Introduction

In the present scenario, the usage of lightweight materials has been increasing to enhance the fuel efficiency in auto-sector. Also, the automobile and aircraft industries are relying on the less weight materials together with the improvements in other mechanical and thermal properties [1]. Also, caused by the growing responsiveness around the ecological disaster and the exhaustion of petroleum possessions, alongside the essential concerns associated with the usability of composite systems [2,3], there is high need to gain maximum optimized benefits from existing inputs. In this regard, the new configurations of composite systems will have to reduce the environmental influence with effectual usage of energy means, materials and waste management [4], development and implementation of new technologies with low

---

influence on the surroundings and, wherever conceivable, substitute synthetic or petroleum materials through sustainable components [5]. Respecting the highly ordinary hybridisation of Carbon fibre reinforced composites materials is very attention-grabbing approach to replace metal applications for the scientific community since the last decade [6].

Carbon fibre reinforced composites are having increased usage due to their excellent performance and lightweight in nature. These composites can be easily, and cost effectively manufactured by compression moulding technique [7]. There is an argument that, carbon fibre reinforced polymers will be the major contributor to about 50% in the aircraft structures in the upcoming years [8]. The interfacial adhesion between the carbon fibre and the polymer matrix governs the final mechanical properties attained [9]. Fibre Metal Laminates are a range of structures that have been used more recently in aircraft fuselage structures and tail panels. More predominantly Glass Aluminium Reinforced Epoxy (GLARE) is used in aircraft structures [1,10,11]. New methods are developed to improve the properties by incorporating natural fibres between these FMLs to make them even stronger [12,13]. Improvement of the performance by adding Carbon Nano tubes and nano clay is underway in many related applications [14,15]. Also, the surface treatments approaches on the aluminium layers are used to progress their mechanical attributes of the FMLs. Studies were carried out for studying the surface morphologies by means of fracture scanning electron microscopy and optical microscopy [16]. FMLs are also recently used as fire resistant materials in aircraft structures. They have used a combination of synthetic and natural fibres. When the mechanical tests are determined, it has been found out that, there is a significant improvement in the performance when natural fibres are combined with them [13]. The mechanical behaviour of the FMLs can be assessed by carrying out compressive, tensile, low-velocity impact, in-plane shear tests [16,17]. One of the significant advantages of FMLs over composite structures is that, if a crack appears on one metal sheet, they are bridged by the other layers that are free from cracks avoiding earlier eruption or failure of the FMLs. Also, the cracks are remaining in the FMLs for a predominantly large period of cycles [18].

Song et al. [19] investigated the impact performance of FMLs based on aluminium and carbon fibres (CARALL) by conducting the experiments and numerical simulations based analysis. The experimental analysis established that the testing samples impacted by 2.35 J reveals no perilous impairment response while the samples impacted by 9.40 J exhibits shear crack on the aluminium surface and failure of fibre and matrix in CFRP layers. Yu at al [20]. investigated the applicability of carbon fibres in FMLs and the influence of the possessions of aluminium alloy on the low-velocity impact retort of CARALL. The simulation outcomes divulge that CARALL exhibits improved impact resistance attributes as compared to GLARE because of better stiffness and strength of carbon fibre reinforced polymer (CFRP). Furthermore, the statistical simulations specified that the impact resistance of CARALL is enriched by raising the yield strength of aluminium alloy. They found that FMLs reveal high resistance to low velocity impact and absorb energy primarily from plastic deformations with glass fibres [21], delamination origination and propagation, however laminates comprising carbon fibres absorb energy due to infiltration and damage [2,22]. The influence of fibre/matrix adhesion on the impact characteristics of carbon FMLs has also been examined [23,24]. Research into resistance to impact is also conducted on FMLS with carbon fibres and different metal layers [25,26]. The Mg/CFRP laminates resulted into significant specific perforation resistance as compared to Al/GFRP laminate [25]. Additionally, titanium/CFRP has better compressive strengths as compared to the composite material even though contains superior impact damage. A study established on the impact performance and damage attributes of hybrid laminates Al/CFRP in contrast to CFRP at low velocity and energy impact [27]. It is established that distinguishing matrix cracks such as bending and shearing cracks are the first damage mode that generate at the interface of fibre/matrix in composite layers [28]. Regardless of the accessibility of investigation on the impact resistance

of FMLs [29], it is very challenging to precisely elaborate the phenomena taking place during impact and the interactions among damages and impact. The developments and process analysis of structural damage of aluminium/carbon composite subsequent from impact are limited and concerned primarily through the examination of the origins of damage origination and propagation observed form of the ultimate damage of FMLs [19].

At extant, there are limited investigations, which stipulate the impact of stacking sequence of metal and fibre layers on the load application in Al6061-FMLs based on carbon fibres throughout impact and the degradation mechanisms. Consequently, targeting to decrease the product final cost deprived of losing the high performance reflected by carbon fibres composites was projected as an attractive consolidation that tolerable not only for the saving of the fabrication costs but also assisted supplementary energy dissipation and damage mechanisms. So, point toward to fill this gap and additional prolong the use of Al6061-FML composites for prime operational and structural applications, the emphasis of this work is to association the ductility of aluminium alloy with the strength of carbon fibres evolving a hybrid system [30]. In detail, the possibility to various sequences of layers of carbon fibre with the metal sheet was examined. Specific consideration is given to the influence of the relative placement of carbon and metal sheets on flexural, and tensile strength, impact and fractographical attributes of the FMLs by designing diverse hybrid configurations.

In the present work we have embedded a systematic research to understand the evolution of the mechanical properties of two altered stacking sequences of FMLs with a carbon fibre reinforced polymer composite. The prime objective was to detect the mechanical properties of aluminium/carbon FMLs manufactured using the novel stacking sequences. Further, the damage initiation and propagation in the examined FMLs were explicitly inferred experimentally and through simulating their respective mechanical conditions. The experiments conducted here allowed to evaluate the tensile strength, impact strength, flexural strength, microstructural evolution, fractographical and surface compositional analysis of Al/CFRP which may lead to massive growth in using this type of material in critical industries.

## 2. Materials and methods

In this method, three different types of specimens were used. They are mentioned herein: out of the three, two were FMLs, which were developed by varying the stacking arrangements. The number of stacks used is five in both the FMLs. They are prepared by having three AA 6061 (A) sheets and two carbon fibre (C) in alternate layers between AA6061, so that the sequence obtained is abbreviated as ACACA (Type - I). In the second type, we have three carbon fibre (C) and only two AA 6061 (A) sheets in alternate layers between the carbon fibre, so that the sequence obtained is abbreviated as CACAC (Type - II). Type – III is a Pure Carbon Composite with seven layers of Carbon fibre.

### 2.1. Carbon fibre

Carbon fibres are today used widely in automotive and aerospace industries where the primary focus is the reduction of the weight and the improving of the fuel efficiency and the mechanical properties too [7,8]. In this work the carbon fibre is used as the reinforcing material and is purchased from a retailer named SM Composites, Chennai. The carbon fibre had a weave pattern of $2 \times 2$ twill and thickness of each carbon fibre layer is also 0.5 mm. The weight per square area is 600 g/m$^2$. It has a temperature resistance up to 260 °C under continuous loading conditions and up to 600 °C for short time temperature resistance. It had an ultimate tensile strength of 774 MPa, the Young's Modulus of the fibre was 59 GPa and the interlaminar shear strength was 51 MPa.

## 2.2. Epoxy resin

For preparing the composite, a thermosetting resin is used, namely Epoxy Resin. It was chosen because of its easier availability and versatility, due to the broad range of properties and processing capabilities. It also has other advantages such as low shrinkage as well as excellent adhesion to a variety of substrate materials such as fillers, fibres and other substances. It has excellent resistance to chemicals and solvents and does not release any volatile matters during curing. In this work the Araldite LY 556 Epoxy resin is used as the matrix material. It is purchased from the same retailer named SM Composites, Chennai. It is having a viscosity of 10,000–12,000 mPa s at 25 °C and its density at 25 °C is in between 1.15 and 1.20 g/cc. The flash point of the resin is greater than 200 °C.

## 2.3. Aluminium 6061 sheet

For developing the Fibre Metal Laminate structures, Aluminium 6061 – T6 sheets were used. Aluminium 6061- T6 is an aluminium alloy whose primary applications are in aircraft and automobile fields. These plates are purchased from a retailer named Coimbatore Metal Mart, Coimbatore. The thickness of the sheets is 0.5 mm. The density of the sheet is 2.7 g/cc. Its ultimate tensile strength is 310 MPa, Yield Strength is 276 MPa and its Modulus of elasticity is around 68.9 GPa. Its shear strength is around 207 MPa.

## 2.4. Development of carbon fibre reinforced composite (type - III)

The specimens were manufactured in a dedicated rubber platen compression moulding machine (100 T) capacity. The machine is capable of giving a pressure of 50 bar. The size of the die used is 150 mm × 250 mm x 4 mm. The composite consists of 5 layers of carbon fibre, each cut to the dimensions of the mould in the die. Then the resin is applied at each layer and after the arrangement of the carbon fibres in the die, the mould is placed inside the compression moulding machine. Once all the individual layers are placed inside the die, the die is closed and it is placed inside the compression moulding machine and a pressure of 50 bar is applied for 8 h or more. Before carrying out the process, the necessary calculations such as mass fraction and volume fraction for both the epoxy resin and fibre material are calculated by using the standard formulas available and from this the ratio of resin and fibre required are determined. Then the resin was properly mixed with the hardener with the proper mixing ratio (10:1). Table 1 shows the various calculations carried out for preparing the carbon fibre reinforced composites. The overall research methodology is shown in Fig. 1. Hand lay-up (Fig. 1(a)) followed by build-up process (Fig. 1(b)), and bonding phase (Fig. 1(c)) includes the development process. Fig. 2 shows the finished carbon fibre composite (Type - III) that has been completed using the compression moulding technique.

## 2.5. Preparation of fibre metal laminate

The Carbon Fibre Metal Laminate structures are prepared by using the same procedure as the one used for preparing carbon fibre composites (as recommended in literature [31]). For this, Aluminium 6061 Sheets are cut to the dimensions of the die, i.e., 250 mm × 150 mm x 4 mm. Then the preparation of the AA 6061 die is carried out in order to

improve its bonding ability with the fibres. Hand abrasion method is opted for surface preparation for interlaminar adhesion as recommended by Lawcock et al. [32], Ostapiuk and Bienias [33], and Sinmazçelik et al. [1]. Usually, AA 6061 sheets have a very fine surface finish at the time of purchase. First, the AA 6061 sheet is roughened using an ordinary scrubbing technique and a metallic wire brush. Then they are mechanically abraded using sandpaper with a grit size of 80 and then it is cleaned with acetone to remove the dust and grease. Then an alkaline etching treatment was carried out by immersing the sample in a NaOH solution (0.2%) for 2 min. If this procedure is not carried out, then the FMLs delaminates easily due to poor surface roughness. Once the sheets are roughened, then they are ready to be stacked in the die. Then the resin is mixed in the proper proportion and the AA 6061 and the Carbon fibre are stacked one over the other alternately with AA 6061 at both ends of the Laminate at one time (ACACA – Type I) and at the next time having Carbon fibre at both ends (CACAC – Type II) of the stack. Once, this procedure is over, they are placed inside the compression-moulding machine for 8 h or more for the FMLs to set. This compression moulding machine helps to ensure the resin transfer is symmetric in all the directions and also prevents the formation of voids. Hence, uniformity in thickness is maintained throughout the preparation of three different configurations of specimens. The following Table 2 indicates the analytical calculations carried out in order to find out the necessary mass fractions and volume fractions required to produce the FML's. Fig. 3 shows the stacking sequence for two types of FMLs used. Fig. 4(a) shows the Carbon Fibre Metal Laminate prepared and Fig. 4(b) shows the cross-sectional view of the Laminate Sandwich. In total four repetitions of experiments are carried out and their standard deviations are calculated which are within desired confidence interval.

## 2.6. Mechanical properties

The following mechanical properties were carried out on the samples. Before carrying out the mechanical tests, all the samples were arranged according to the ASTM standards. All the mechanical tests were carried out at "METMECH ENGINEERS", Chennai, an authorised mechanical testing centre for carrying out various performance evaluations of composites and metallurgical components.

### 2.6.1. Tensile test

Tensile testing is one among the important tests which is carried out frequently in most of the cases during material characterization. It is a test which helps to determine, how far the sample is capable of withstanding, when it is subjected to an axial pull. Fig. 5(a) shows the ASTM D 638 standard for performing the tensile tests. Fig. 5(b) shows the samples prepared as per the above standards. The maximum tensile load of 5 kN was applied during the test. The equipment used for carrying out the tensile test is HAIDA Tensile Testing Machine, HD-B615A-S, a China made machine available at the testing centre. It can give loads in varying range from 5000 N to up to 50 kN. The vertical test space is about 1000 mm.

### 2.6.2. Impact test

Impact test is a test able to determine the behaviour of a material under sudden impact load. It helps to find out the maximum amount of energy absorbed by the material before the material fails. It tells how tough the material is. Fig. 6(a) shows the ASTM D 256 standard used for

**Table 1**
Analytical calculation for carbon fibre composite.

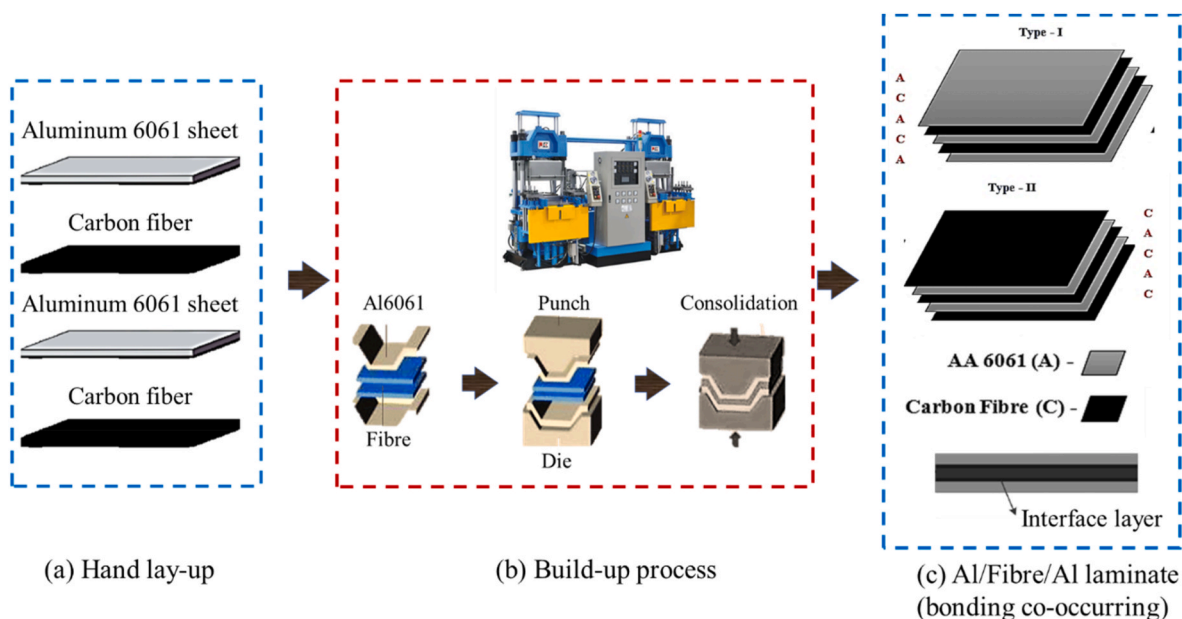| Type | Volume of Composite (mm$^3$) | Volume Fraction | | Mass (gm) | Mass Fraction | | Density (kg/m$^3$) | Young's Modulus (GPa) | | Poisson's Ratio | | Shear Modulus (GPa) |
|------|---|---|---|---|---|---|---|---|---|---|---|---|
| **Carbon Composite** | 190625 | **Fibre** | 0.344 | 297.9625 | **Fibre** | 0.4965 | 1563.081 | $E_x$ | 10.578 | $\mu_{12}$ | 0.3195 | 1.6853 |
| | | **Matrix** | 0.6557 | | **Matrix** | 0.5034 | | $E_y$ | 4.959 | $\mu_{21}$ | 0.1497 | |

**Fig. 1.** Experimental schematic illustration of Carbon fibre metal laminate: (**a**) Hand lay-up, (**b**) Build-up process, and (**c**) Al/Fibre/Al laminates.
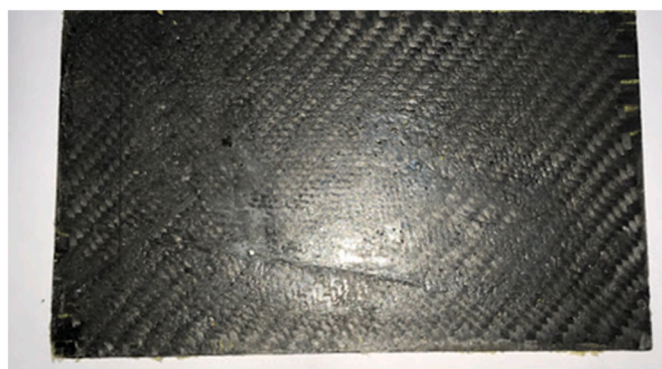


**Fig. 2.** Carbon fibre composite prepared.

preparing the samples for impact test. Fig. 6(b) shows the samples prepared accordingly. The equipment used for carrying out the impact testing is a China made Analog CZT3250 izod and Charpy tester. It is having a maximum capacity of 50 J. The raising angle is about 150°. It has an impact centre distance of 395 mm.

*2.6.3. Flexural test*

Flexural test is used to determine the flexural strength of the material investigated. It helps to determine the materials ability to resist deformation under load in which the load is applied perpendicular to the longitudinal axis of the material. A 3-Point Bending test was carried out. Fig. 7(a) shows the ASTM D 790 standard used for preparing the samples

needed for carrying out the flexural tests. Fig. 7(b) shows the samples prepared as per the standards. The testing equipment used for carrying out 3-point bending test is Flexure Fixture, Instron Made, America. It is capable of giving loads up to 5 kN. It has a maximum and minimum span of 194 mm and 4 mm respectively. The diameter of the upper anvil is 10 mm. The operating temperature is −100 °C to +350 °C.

## 3. Microstructural investigation, and energy dispersive X-Ray analysis

Microstructural investigation is a method used for finding out the magnified image of the object under study and to find the surface properties of the samples. It is a very excellent method for finding out even smaller variations and irregularities in the materials used in the samples. Further, the microstructural investigation was carried out before and after the mechanical tests in order to find out some differences in the fractography. The samples are cut to the dimensions of 10 mm × 10 mm. For carrying out the microstructural investigation, surface must be free from dust particles and other foreign matter. Therefore, firstly the samples are properly cleaned using alkaline solutions, then they are dried. After that they are exposed to the SEM analysis. The SEM images are taken from International Research Centre, Kalasalingam University, Krishnankovil. The equipment used for carrying out SEM is a German Made Scanning Electron Microscope EVO18 (CARL ZEISS). It is having a resolution of 50 nm, angular tilt of 0–60° and 360° rotation. The magnification can vary from 50000 to 100000 times depending upon the sample. The three different types of samples used for the investigations are shown in the following Fig. 8.

**Table 2**
Analytical calculation for Fibre Metal Laminates.

| Type | Volume of Composite (mm$^3$) | Volume Fraction | | Mass (gm) | Mass Fraction | | Density (kg/m$^3$) | Young's Modulus (GPa) | | Poisson's Ratio | | Shear Modulus (GPa) |
|---|---|---|---|---|---|---|---|---|---|---|---|---|
| **ACACA (Type - I)** | 2291566.66 | **Reinforcement** **Matrix** | 0.33635 0.67272 | 249.976 | **Reinforcement** **Matrix** | 0.25991 0.7400 | 1090.8 | $E_x$ $E_y$ | 10.1793 4.8387 | $\mu_{12}$ $\mu_{21}$ | 0.25849 0.4753 | 1.8214 |
| **CACAC (Type - II)** | 219791.66 | **Reinforcement** **Matrix** | 0.2985 0.7014 | 263.5465 | **Reinforcement** **Matrix** | 0.298 0.7019 | 1199.074 | $E_x$ $E_y$ | 8.636 4.655 | $\mu_{12}$ $\mu_{21}$ | 0.2597 0.1399 | 1.769 |
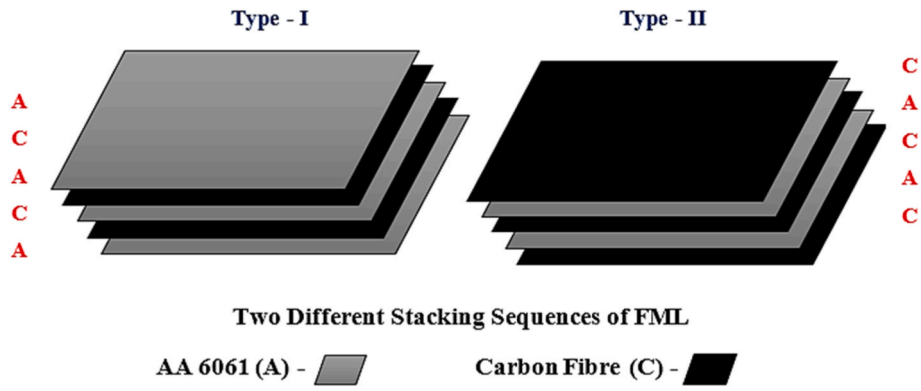
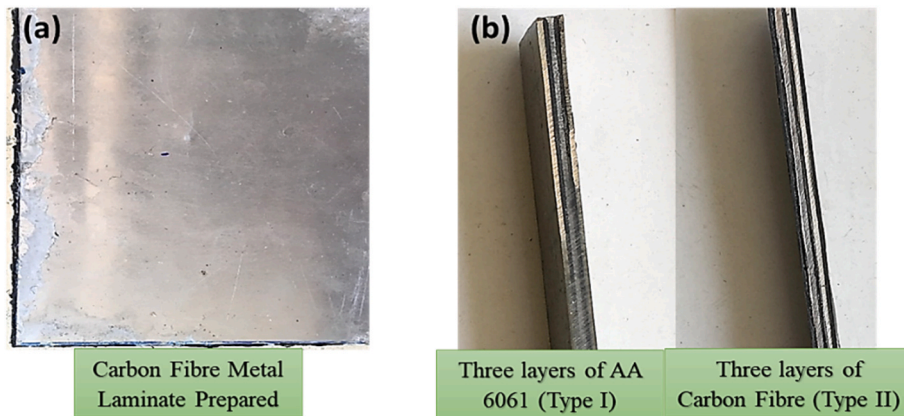**Fig. 3.** Stacking sequence for two types of FMLs.



**Fig. 4.** Carbon Fibre Metal Laminate Prepared: (**a**) top view, and (**b**) cross-sectional view of Laminate Sandwich.
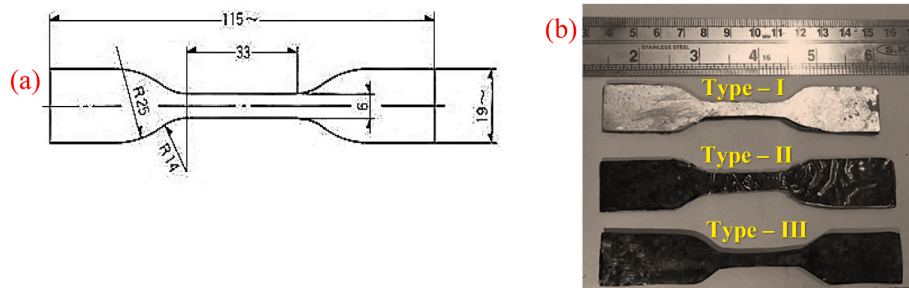


**Fig. 5.** (**a**) Tensile specimen schematic as per ASTM D 638 standard, and (**b**) prepared specimens for tensile testing.
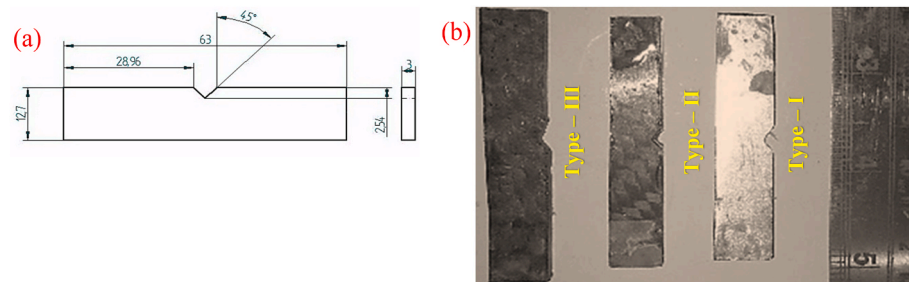


**Fig. 6.** (**a**) Impact test specimen schematic as per ASTM D 256 standard, and (**b**) prepared specimens for impact testing.

## 4. Numerical simulation

In the present work, Numerical Simulation is carried out in order to validate the experimental results obtained from tensile and flexural tests. Abaqus 6.14–1 has been used as an analysis tool to carry out the simulation process. The Johnson-Cook plasticity model for their
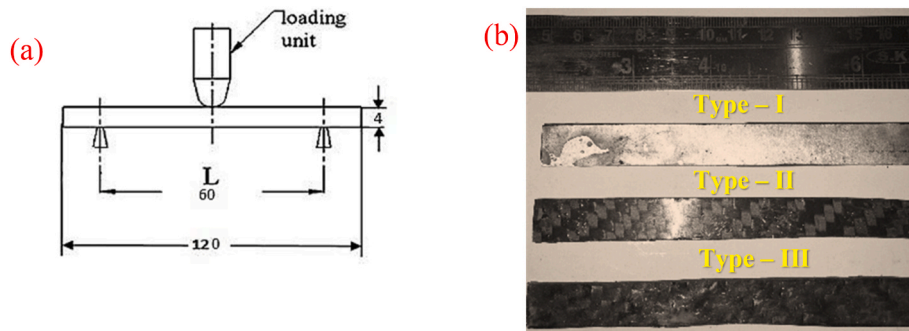
**Fig. 7.** (**a**) 3-Point Bending test schematic as per ASTM D 790 standard, and (**b**) prepared specimens for flexural testing.
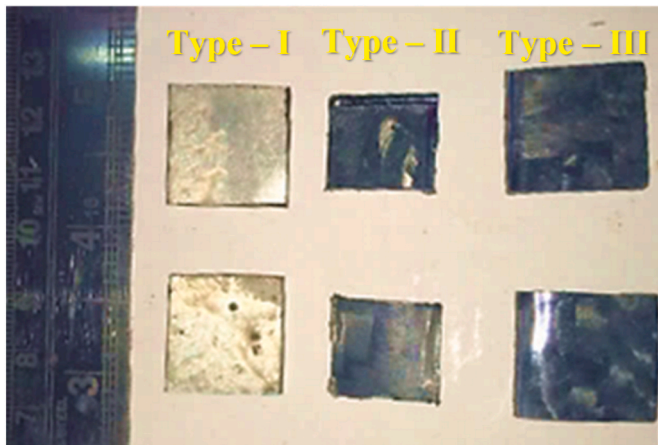


**Fig. 8.** Samples prepared for SEM analysis.

numerical simulation process has been emplyeed. A model having similar dimensions as that of the tensile and flexural specimen has been created in the part module of Abaqus. The dimensions of the tensile and flexural specimens required are shown in Figs. 5(a) and Fig. 7(a) respectively. Here the purpose is to find out the stress variation in the specimens during tensile tests and also to find out the maximum y-directional displacement during flexural tests. Then these results are correlated with the experimental data. The type of analysis carried out is Dynamic Explicit. The model has been generated with individual elements as in TYPE-I, TYPE-II and TYPE-III. The individual components are modeled with a thickness of 0.5 mm and they are stacked together to depict the actual model. The property values given as input are shown in the following Table 3 and Table 4.

Above Tables 3 and 4 are given as property inputs in ABAQUS for AA6061 and Carbon fibre respectively. The model has been simulated by carrying out the simulation process in Dynamic Explicit with a step time of 0.001. Proper interaction has been given as input in order to depict the actual resin cohesive behaviour in between the resin and the composites. Load values are given as given in Table 5. Fig. 9 and Fig. 10 show

the assembled view of the Type-I FML.

During the process of Meshing, AA 6061 and Carbon Fiber has been given the element type with the following inputs as shown in Table 6.

The type of element chosen for AA 6061 is C3D8R: An 8-node linear brick, reduced integration, hourglass control. It is modeled with Hex-Sweep Mesh. The type of element chosen for Carbon Fiber is SC8R: An 8-node quadrilateral in-plane general-purpose continuum shell, reduced integration with hourglass control, finite membrane strains. It is also modeled with Hex-Sweep Mesh. Fig. 11 shows the Load applied and boundary conditions during the simulation process. The meshed view of the model is shown in Fig. 12.

In the same way, Fig. 13(a) shows the geometry and boundary conditions used for carrying out flexural test. Fig. 13(b) shows the meshed view of the geometry. A total of four components were used and they are assembled. Out of these four, three of the cylindrical components are made as discrete rigid. The necessary time increment is given in the step module. The values for input have been taken from the experimental data and those depicted in Tables 3 and 4 A Static, General analysis was carried out and the element type chosen for this analysis is C3D8R.

## 5. Results and discussions

### 5.1. Tensile strength analysis

The tensile test results for the samples are shown in the following Table 7. From the table, the tensile strength of Type – I material is 192.92 MPa, whereas it is about 155.83 MPa for Type – II and 145.83 MPa for Type – III material. By taking Type – III as a reference material, since we are comparing FML with composite, Type – I is fairly around 24.40% higher than Type – III and Type – II is 6.41% higher than Type - III. Again, the amount of tensile load withstanding capacity for Type – I material (4.66 kN) is around 20.17% higher than Type – III (3.72 kN) and for Type – II (3.74 kN) it is only about 0.534% higher than Type – III (3.72 kN). From these results it can be identified that Fibre Metal Laminates are having better load withstanding capacities when compared to carbon fibre reinforced composites. This is because pure carbon fibre has a homogeneous material content, whereas both the

**Table 3**
Property values for AA6061 for Abaqus Simulation.

| AA6061 | | | | | | | |
|---|---|---|---|---|---|---|---|
| 1. | Ductile Damage | Fracture Strain 32.66 | Stress Triaxiality −0.47 | Strain Rate 0 | | | |
| 2. | Damage Evolution | Fracture Energy (Nmm) 656.466 | | | | | |
| 3. | Density (Kg/mm$^3$) | 2.78e-6 | | | | | |
| 4. | Elastic | Young's Modulus (N/mm$^2$) 68900 | Poisson's Ratio 0.33 | | | | |
| 5 | Plastic (Johnson-Cook) | A 324.1 | B 113.8 | n 0.42 | m 1.32 | Melting Temperature 925 | Transition Temperature 293.2 |

**Table 4**

Property values for Carbon Fibre for Abaqus Simulation.

| Carbon Fibre | | | | | | | | | |
|---|---|---|---|---|---|---|---|---|---|
| 1. | Hashin Damage | Longitudinal Tensile Strength (N/mm$^2$) | Longitudinal Compressive Strength (N/mm$^2$) | Transverse Tensile Strength (N/mm$^2$) | Transverse Compressive Strength (N/mm$^2$) | Longitudinal Shear Strength (N/mm$^2$) | Transverse Shear Strength (N/mm$^2$) | | |
| | | 1800 | 1200 | 40 | 180 | 70 | 40 | | |
| 2. | Damage Evolution | Longitudinal Tensile Fracture Energy (Nmm) | Longitudinal Compressive Fracture Energy (Nmm) | Transverse Tensile Fracture Energy (Nmm) | Transverse Compressive Fracture Energy (Nmm) | | | | |
| | | 12500 | 12500 | 2500 | 2500 | | | | |
| 3. | Damage Stabilization | Viscosity Coefficient in Longitudinal Tensile direction | Viscosity Coefficient in Longitudinal Compressive direction | Viscosity Coefficient in Transverse Tensile direction | Viscosity Coefficient in Transverse Compressive direction | | | | |
| | | 0.0007 | 0 | 0.001 | 0 | | | | |
| 4. | Density | 1.6e-6 (Kg/mm$^3$) | | | | | | | |
| 5. | Elastic – (Engineering Constants) | E1 (N/mm$^2$) | E2 (N/mm$^2$) | E3 (N/mm$^2$) | Nu12 | Nu13 | Nu23 | G12 | G13 | G23 |
| | | 130000 | 10000 | 10000 | 0.28 | 0.28 | 0.5 | 4500 | 4500 | 3500 |

**Table 5**

Input parameters for numerical simulation for tensile, and flexural Test.

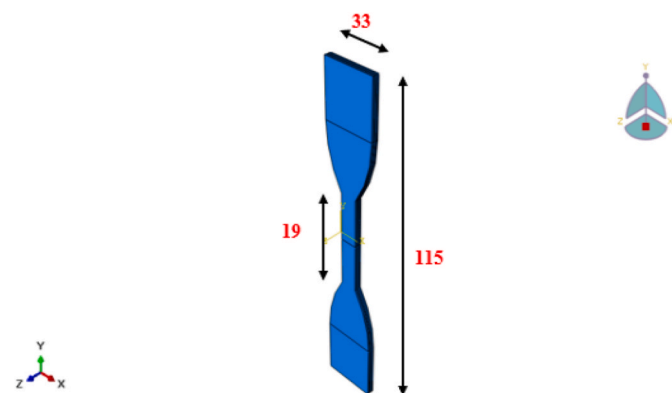| Test | Type | Maximum Displacement (mm) | Load (N) | Maximum Yield Stress | Plastic Strain |
|---|---|---|---|---|---|
| Tensile | Type – I | 11.43 | 4660 | 259.47 | 0.2644 |
| | Type – II | 10.05 | 3740 | 103.82 | 0.2538 |
| | Type - III | 9.28 | 3720 | 278.12 | 0.2215 |
| Flexural | Type – I | 11.1 | 40 | – | – |
| | Type – II | 8 | 25 | – | – |
| | Type - III | 2 | 155 | – | – |



**Fig. 9.** Assembled view of Type-I FML.

types of FMLs have varying material content along the matrix and further carbon fibre composites will normally fail due to brittle fracture. Moreover, the percentage elongation for Type – I (28.57%) is far better than the one of the two specimens. This proves that Type – I (FML) could be capable of sufficiently withstanding the maximum loads before failure takes place. This makes it advantageous to be chosen as a material for aircraft structures.

The numerical simulation has been used as a tool for validating the experimental results obtained from the tensile and flexural tests. Fig. 14 (a) shows the stress vs strain curve for Type – I specimen correlated with

numerical values. Similarly, Fig. 14(b) and (c) shows the stress vs strain curves correlated for Type – II and Type – III specimens respectively. Fig. 14(d) shows the Von-Mises stress plot for Type – I specimen. It can be clearly visualised that the stress applied is very high at the centre of the specimen. Numerical simulation using Abaqus 6.14–1 gives fairly good results in accordance with the experimental data. The maximum value of tensile strength obtained from numerical simulation is about 194.158 MPa, 155.829 MPa and 148.565 for Type – I, II and III respectively. On taking the percentage deviation of the experimental results and the Abaqus output into account, it can be seen from the graph that for Type – I specimen, it is only around 0.63%. Similarly, for Type – II specimen, it is about 0.0024% which is the minimum and for Type – III specimen it is about 1.83%. This smaller deviation in the final output from the numerical simulation values may be caused due to the variations in step time, mesh size and loading conditions given. Careful considerations have been taken to minimize these errors during simulation process.

Further taking the failure into account, Type – I and Type – II specimens shows failure, which are more or less equal to ductile mode. But when compared with pure composites and monolithic aluminium, this failure is found to lie between these two. Hence, it takes the advantages of both. But, on the other hand, in case of Type – III, it can be seen that the failure taking place is purely a brittle failure, because composites are purely brittle in nature. This is the major difference that differentiates a composite from a fibre metal laminate. For example, if a composite structure is used in aircraft panels, and in some cases if failure takes place, then there is a sudden fracture taking place because of brittle failure. But on the other hand, since a Fibre Metal Laminate has the sum of the combined properties of these two separate components (aluminium and composite structures), it fairly behaves like ductile and brittle failure and hence the time taken for the complete destruction is satisfactorily extended. This is the greatest advantage with fibre metal laminates [17,18]. It can also be seen that the strain rate of Type – I FML is about 28.01% higher than that of Type – III composites and for Type – II specimen it is about 18.11% higher than Type – III composites [34]. This gives us an evidence that, the FMLs are capable of allowing the AA 6061 sheets to extend beyond the individual strain rate of monolithic aluminium sheet.

Figures 15–17 show the displacement plot output of the tensile test for Type-I FML, Enlarged View of the Simulated output of tensile test for Type-I specimen and cut-section view of Y-displacement plot showing the delamination taking place due to the application of tensile load for Type-I FML. It can be visualised that the breaking of the FML is taking place at the centre of the specimen.

Fig. 18(a) shows the specimens after conducting the tensile tests. It

**Fig. 10.** Top view showing the individual components stacked together for Type-I FML.

**Table 6**
Details of input for meshing the components.

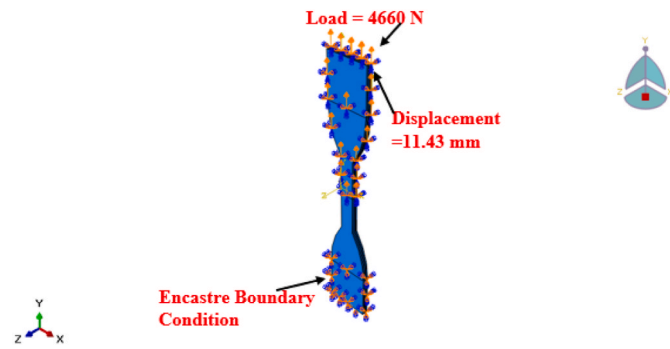| Material | Element Library | Family | Geometric Order |
| --- | --- | --- | --- |
| AA 6061 | Explicit | 3D Stress | Linear |
| Carbon Fiber | Explicit | Continuum Shell | Linear |



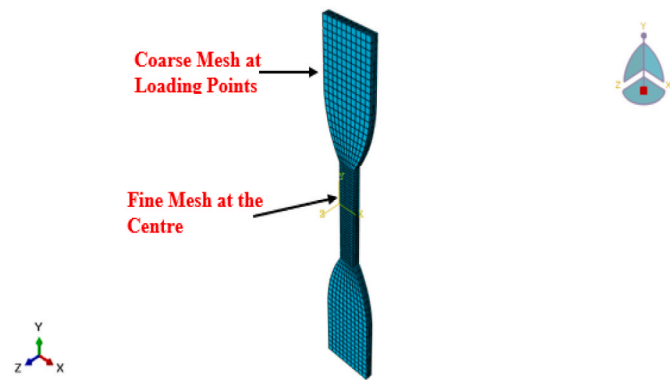**Fig. 11.** Load and boundary conditions applied for Type-I FML.



**Fig. 12.** Meshed view of Type-I FML.

can be visualised that in Type – I and Type – II specimens, the failure has taken place exactly at the centre of the specimen and in Type – III it is away from the centre due to brittle nature of composites. During the testing of FMLs after the load has gone beyond the elastic limit, there occurs delamination of the AA 6061 sheets and a ticking sound is heard. On further application of load only, there is failure of the carbon fibre, whereby it results in the complete failure of the specimen [35]. Hence, it resulted that there is an additional load bearing capacity from the AA 6061 sheets, which supports and prevents the initial damage to the fibre taking place due to the application of load, and in turn helps to extend the time of failure of the entire specimen. But, on the other hand, in case of Type – III carbon composites, the failure takes place suddenly without any sign of the crack initiation, as it is a brittle material. Fig. 18(b) shows the ultimate tensile strength for three types of specimens. It can be seen from the graph that Type – I specimen achieves a maximum Tensile Strength of 192.92 MPa.

### 5.2. Impact strength analysis

The impact test results were shown in the following Table 8. It can be seen that the value of the impact test is higher for Type – I specimen with 9.3 J and it is lower for Type – III with 1.9 J and has the mid value of 5.2 J for Type – II specimen. Fig. 19(a) shows the variation of the impact values with respect to the variation in the type of specimens used. Here, we can clearly observe that, the impact value is larger for Type – I specimen as desired. This confirmed the capability of the FML in withstanding a very good impact resistance [12,13,17]. Type – II FML has carbon fibre at the outer end, but even though increases the impact resistance is still not fair enough. Further taking Type – III as a reference, it can be seen that the impact value of Type – I specimen is 79.56% more than Type – III and impact value of Type – II specimen is 63.46%, more than Type – III. Fig. 19(b) shows the specimens after the impact tests. It can be seen that a delamination of the FML specimens occurs when they are subjected to impact load. The load is completely absorbed by the FML itself, leaving no damage to the neighbouring parts or to the humans nearby. For Type – III specimen the impact load results in the damage of the area where the notch has been created [36].

### 5.3. Flexural strength analysis

The flexural test results for the three types of specimens are shown in the following Table 9. It is seen that the ultimate breaking load is around 155 N for Type – I, 120 N for Type – II and 75 N for Type – III. When maximum displacement is taken into account, it is 11.10 mm for Type – I specimen before the failure takes place. For Type – II specimen it is around 8 mm and for Type – III specimen it is only 6.30 mm. It can be noted that in flexural testing also Type – I specimen is capable of withstanding maximum displacement before it is prone to failure when compared to the other two types. The following Fig. 20(a) shows the ultimate breaking load for three types of specimens. The ultimate breaking load for Type – I specimen is about 155 N.

During the tests, it can be observed from Fig. 20 (a) that Type – I FML is capable of withstanding fluctuating loads before failure takes place. Initially, it takes a load nearly equal to 155 N and then due to the result of delamination in the specimen, it starts decreasing its load holding capacity to around 123 N. But as the time increases, as well as the load, once again the peak rises to around 140 N and it starts delaminating at a faster rate. Finally, it is no more able to withstand the load before complete failure occurs. Now considering Type – II, FML is capable of
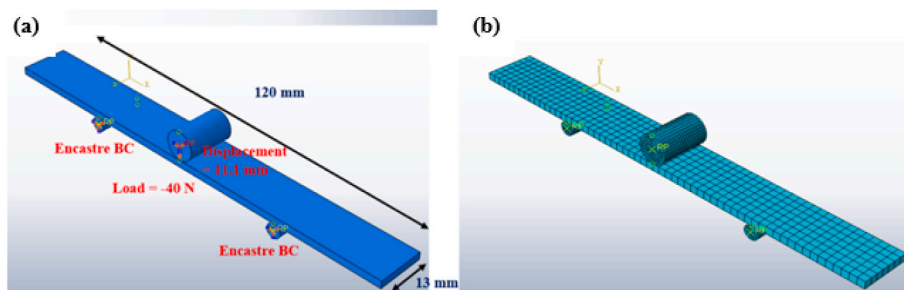
**Fig. 13.** Numerical simulations: (**a**) geometry and boundary conditions for flexural test, and (**b**) meshed view of the model for flexural test sample.

**Table 7**
Results of tensile tests.

| S. No. | Sample: | Tensile Strength (MPa) | Standard Deviation (MPa) | Maximum Strain (%) | % Elongation | Tensile Load (kN) | Maximum Displacement (mm) |
|---|---|---|---|---|---|---|---|
| | Type – I | 192.92 | 1.25 | 32.66 | 28.57 | 4.66 | 11.43 |
| | Type – II | 155.83 | 1.12 | 28.71 | 20 | 3.74 | 10.05 |
| | Type – III | 145.83 | 1.71 | 23.51 | 20 | 3.72 | 9.28 |
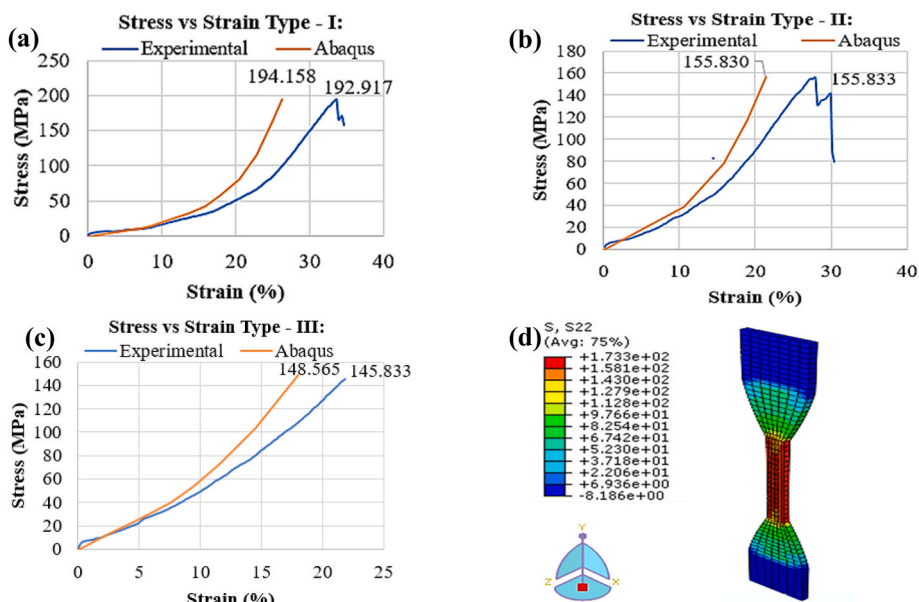


**Fig. 14.** Stress Vs Strain curves verified against Abaqus for (**a**) Type – I, (**b**) Type – II, (**c**) Type – III Specimens, and (**d**) Von-Mises stress plot of Type - I.

initially supporting a load of around 120 N but as the loading increases, it starts falling along the displacement axis and on further application of load it rises to a value of around 110 N and after which the deformation is permanent due to delamination of the specimens.

Considering Type – III it is possible to note that at the first step the load starts raising steadily up to 75 N and then decreases slightly. Then once again rises to 60 N but then immediately starts decreasing its load withholding capacity and finally destroys at 30 N. Fig. 20(b) shows the specimens after flexural tests. It is observed that Type – I and Type – II specimens are delaminated and the amount of displacement taking place is large before failure takes place. In case of Type – III, even though it is capable of withstanding larger load compared to the former two types, still the failure taking place is sudden without any prior information amount the cause of failure. This is due to the brittle nature of the composites, despite the FMLs which combine both ductile and brittle fracture, overcoming this disadvantage [37].

Further, the numerical validation of the flexural tests has been done using Abaqus 6.14–1. The following Fig. 21(a) shows the maximum displacement in the Y-direction obtained during the numerical simulation. The corresponding comparison graph for the experimental and numerical values is shown in Fig. 21(b). It can be seen that the percentage deviation in the output displacement is around 11.66% for Type – I specimen, and 8.46% for Type – II specimen and it is around 6.16% for Type – III specimen. This deviation in the output is due to the mesh size, the step time given, and the experimental conditions applied during the simulation process. This once again gives fairly good results in accordance with the experimental data obtained during the flexural tests.

### 5.4. Microstructural evolution

Fig. 22(a–d) show the microstructure of pure carbon composites at various magnifications of 50X, 500X, and 2000X. In Fig. 22(a) the surface is smoother at some areas and in some locations, it has rough surfaces. Where there are rough surfaces, the fibres running from one end to the other is visible.

In Fig. 22(b) the orientation of the fibre appears along the longitudinal direction. From Fig. 22(c) the white particles sticking to the
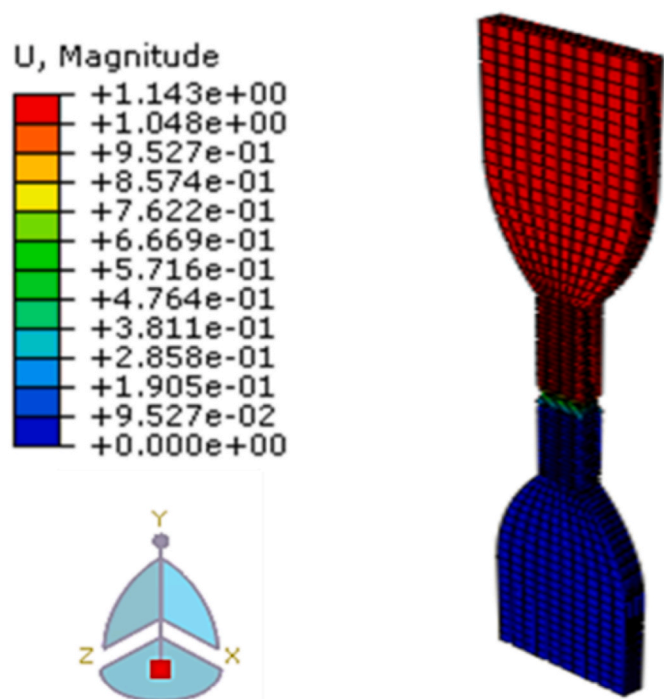
**Fig. 15.** Simulated output of tensile test using ABAQUS 6.14–1 for Type-I specimen.
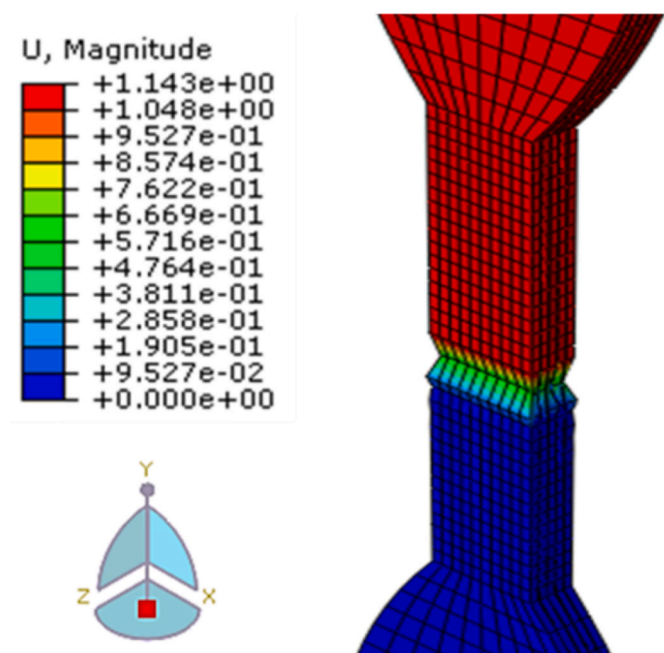


**Fig. 16.** Enlarged view of the simulated output of tensile test using ABAQUS 6.14–1 for Type-I specimen.

surface of the fibres is inferred. These are epoxy resin particles which are agglomerated at certain areas due to poor pressure applied over the zone at the time of manufacturing. When the magnification is increased to around 2000 times as in Fig. 22(d), some of the pores are developed in the composites. This is due to insufficient resin at the top surface, creating these voids. Some of the damaged fibres at the top surface are visible. These are nothing but the small, chopped fibres fallen during the time of composite manufacturing.

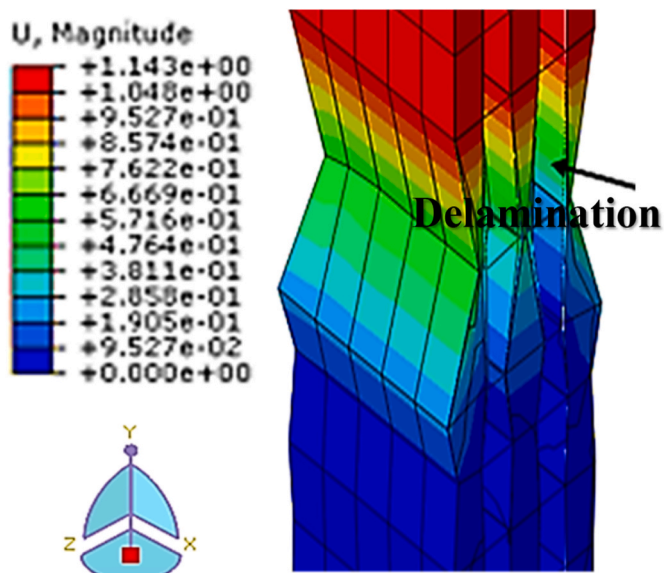Fig. 23(a–d) show the microstructural investigation carried out on



**Fig. 17.** Cut-section view of Y-displacement plot showing the delamination taking place due to the application of tensile load for Type-I FML.

Type – I FML at various magnifications of 50X, 150X, 500X and 2000X, respectively. Fig. 23(e) shows the particle size of the carbon fibre at a magnification of 3000X. In these figures, we can see the arrangement of FML consisting of AA6061 plates at the outer end (Type-I), subsequently followed by carbon fibre on alternate layers. In Fig. 23(a) we can see that there are a total of 5 layers or laminate with 3 numbers of AA6061 plates and 2 numbers of carbon fibre between them. In this figure a layer which consists of a small gap in the FML appears. This is due to the variation in the thickness of the carbon fibre layer. Also, the defect raises because of scarce of matrix phase in this region. This may lead to poor strength of the joints produced. But under normal visual inspection, this cannot be seen by our naked eyes. In Fig. 23(b) the magnification is increased to 150X and the line of joining of the two materials exists and it proves that the joining is very perfect here. On further subsequent magnifications of 500X Figs. 23(c) and 2000X Fig. 23 (d), the joining seems perfect and the gaps in the AA6061 sheet is being filled by the carbon fibres and the adhesion is achieved due to the matrix. In Fig. 23(e) the magnification is increased to 3000X. All the fibres are oriented in the same direction, in this case perpendicular to the page. The diameter of the fibres is measured using the SEM apparatus at Kalasalingam University, Krishnankovil. Two individual fibre leaves are selected and both showed the same diameters of 6.348 μm (Pa 1, and Pa 2).

### 5.5. Fractographical analysis

Fig. 24(a) and Fig. 24(b) shows the fractographical investigation carried out in the tensile tested specimens of Carbon fibre composite. The focus is at the place where the tensile failure has taken place. Due to the pull force applied to the end of the specimens, the component failure has resulted in the elongation of the fibres at the centre and some of the fibres are pulled out from their actual position and some were even broken. Many deep valleys resulted created on the failure zone of the composites. On higher magnification, is clearly visualised the arrangement of fibrous bundles of the carbon fibre. Between the fibrous bundles, we can also see some void gaps formed due to scarce matrix material.

In the same way, the fractographical investigation has been carried out on the tensile tested Type – I FML specimen. Fig. 25(a–e) shows the areas where the tensile failure has taken place with various magnifications of 50X, 50X, 100X, 250X, and 500X, respectively. In Fig. 25(a) the specimen after failure is seen in the form of a step. Since the carbon fibre used here is a woven mat, it consists of fibres running along both
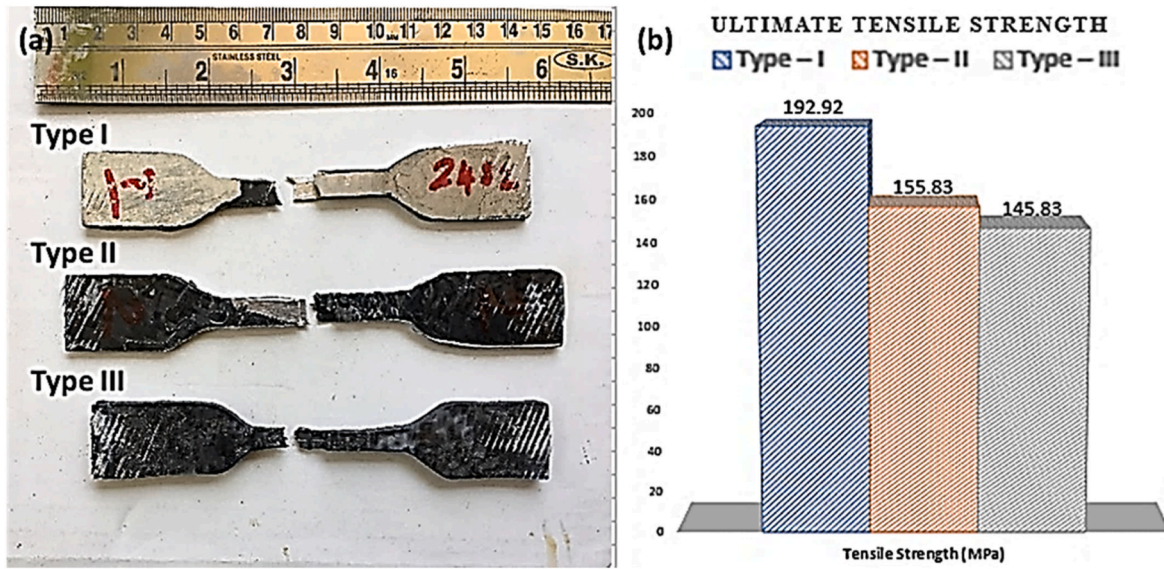
**Fig. 18.** (**a**) Fractured tensile specimens, and (**b**) Ultimate tensile strength for three types of specimens.

**Table 8**
Results of impact tests.

| S. No. | Specimen Type | Impact Energy (J) | Standard Deviation |
|---|---|---|---|
| 1. | Type – I | 9.3 | 0.94 |
| 2. | Type – II | 5.2 | 0.62 |
| 3. | Type – III | 1.9 | 0.83 |

perpendicular directions. And due to this we can see in Fig. 25(b), that fibres are seen running horizontally as well as perpendicularly. There are some voids which are formed due to imbalance flow of matrix inside the FML. On further magnification in Fig. 25(c), some of the pulled-out fibres are identified due to the applied tensile force. Sheet of fibres running perpendicularly are visualised in Fig. 25(d). Further some ridges and valleys are also seen in the microstructure due to the emptiness created by certain volume of material removed there. In Fig. 25(e), AA6061 has some serrations in it due to the tensile failure. Fibrous bundles that are running horizontally are very clearly visible in this image.

### 5.6. Surface compositional analysis

The main purpose of carrying out EDX analysis is to find out whether there is any formation of chemical components other than that of the base materials used. The EDX analysis for two-specimen viz. Type – I and Type – III have been carried out. Fig. 26(a) and Fig. 26(b) shows the EDX analysis carried out on the Type – III specimen. There are two peaks seen in the image, which gives the weight percentage of carbon (66.88%) and Oxygen atoms (33.12%). The rest of the peaks indicate other elements that are negligible. The presence of oxygen atoms is due to the contact with the atmosphere. There are no additional compounds formed expect

**Table 9**
Results of flexural tests.

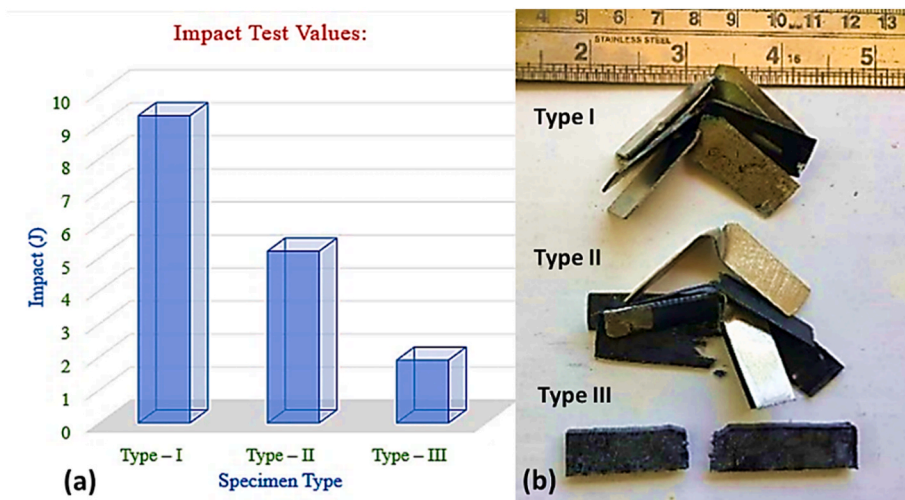| S. No. | Specimen Type | Ultimate Breaking Load (N) | Standard Deviation | Maximum Displacement (mm) | Ultimate Stress (kN/mm$^2$) |
|---|---|---|---|---|---|
| 1. | Type – I | 155 | 3.75 | 11.10 | 0.003 |
| 2. | Type – II | 120 | 2.01 | 8.00 | 0.001 |
| 3. | Type – III | 75 | 1.88 | 6.30 | 0.001 |



**Fig. 19.** (**a**) Impact energy values with each type, and (**b**) specimens after impact tests.
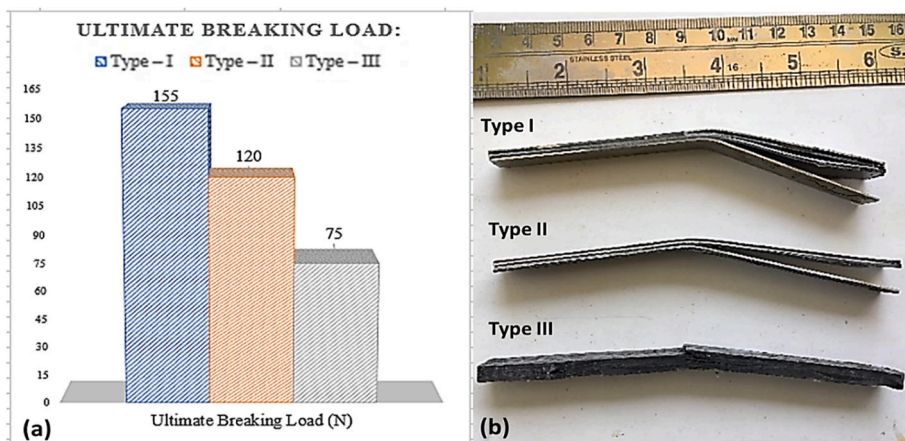
**Fig. 20.** (**a**) Ultimate breaking load for three types of specimens, and (**b**) specimens after conducting flexural tests.
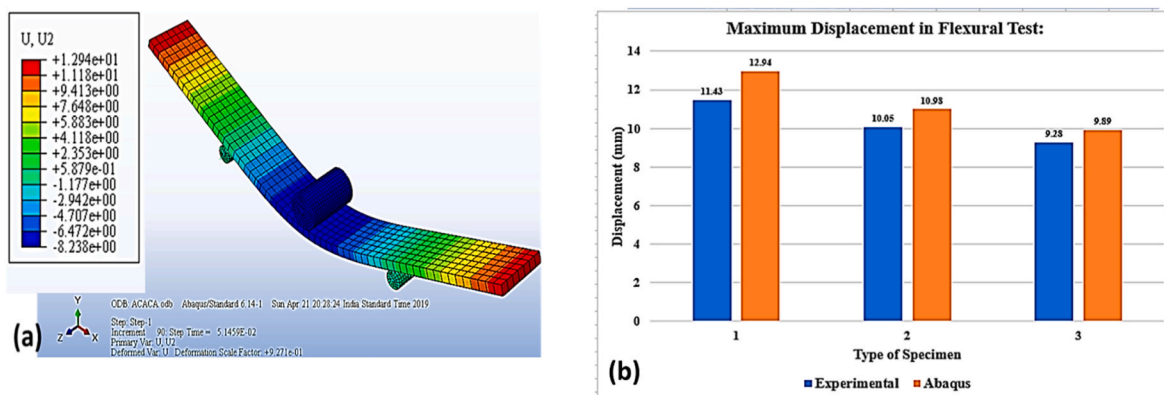


**Fig. 21.** (**a**) Maximum displacement plot for Type – I specimen, (**b**) comparison of experimental and numerical values of flexural displacement.
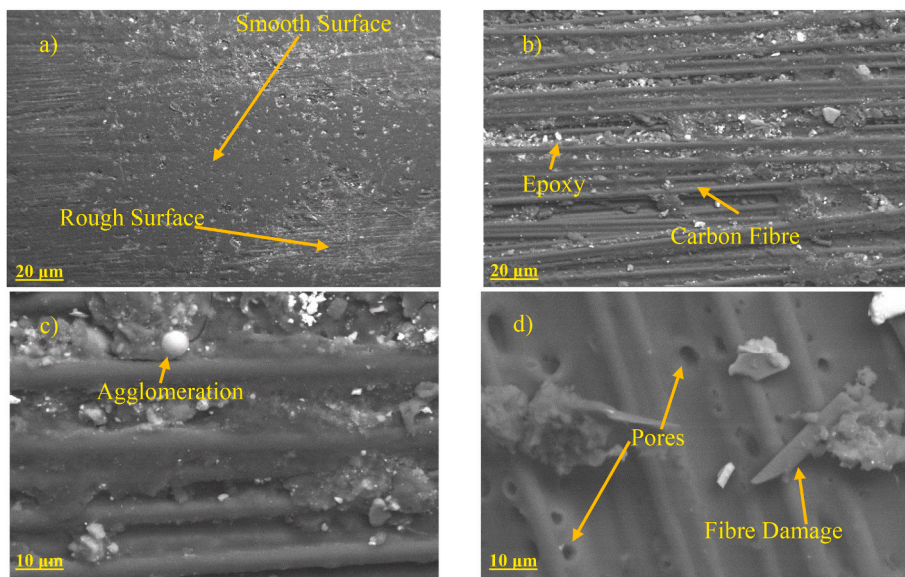


**Fig. 22.** Microstructure of Carbon fibre composites at various magnifications: (**a**) surface features, (**b**) epoxy and carbon fibre, (**c**) evolution attributes, and (**d**) surface defects.

oxygen.

Similarly, the EDX analysis on the FML is carried out at three places as shown in Fig. 27(a): one exactly at the centre, one at the area of

carbon fibre and one at the AA6061 side. It can be seen from Fig. 27(b) that, there is a combination of both Carbon Fibre and AA 6061 at the centre having weight percentages as 52.68% and 47.32%. This shows
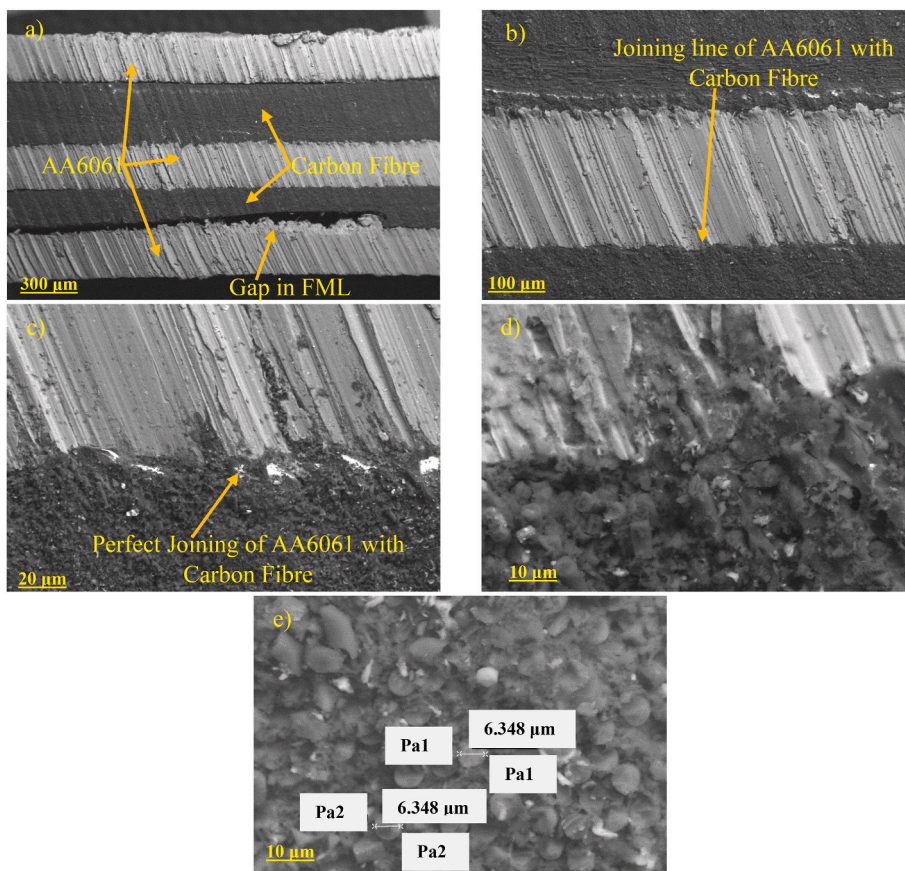
**Fig. 23.** Microstructure of Fibre Metal Laminates at various magnifications: (**a**) cross sectional view, (**b**) magnified view, (**c**) joining mechanism, (**d**) magnified view of joining mechanism, (**e**) size of Carbon Fibre.
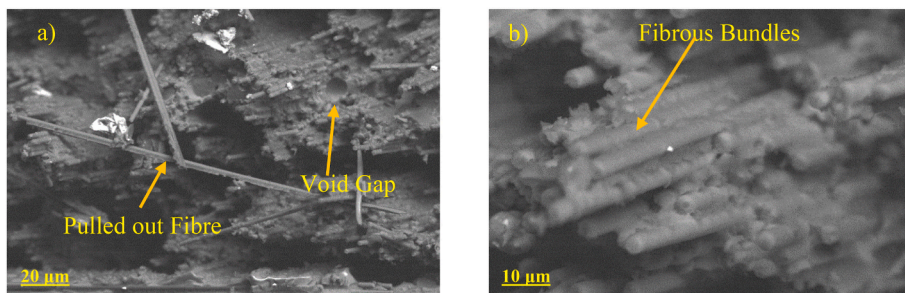


**Fig. 24.** Fractography of Carbon Fibre Composites at the failure Zone (**a**) fractured surface, and (**b**) surface evolution.

that at this analysis point there is perfect merging of the two materials namely AA 6061 and carbon fibre. In Fig. 27(c), the point of focus is on AA 6061 side; so, there is a peak of 82.25% AA 6061 atoms by weight and still there is a small percentage of carbon in it having a weight percentage of 15.79% with Oxygen atoms 1.95%. There is no evidence of any third compound formation. In the same way, in Fig. 27(d) where the analysis is on carbon fibre side, there is a peak rise of 79.96% carbon, 16.58% Oxygen atoms and 3.46% AA 6061 atoms by weight. This proves that the joint formed is perfect and the bonding between the carbon fibre and AA 6061 sheet is good. Here also, there is no evidence of any third new compound formation.

## 6. Conclusions

The focus point of this work was to find a material that would be helpful in improving the performance of the aerospace component

structures. Hence, they are prepared as per the necessary sequence and their mechanical properties are envisaged. Form the results obtained.

- It is proved that even though carbon fibre composite is having excellent mechanical properties, yet its brittle nature is an obstacle to the material science engineers. Hence, FMLs are chosen today in most of the applications wherever necessary. This FML combines the advantages of conventional ductile Aluminium sheets and also the brittle composites. Hence, the combined effect has helped the engineers to choose it as an excellent material for aerospace application. These materials have shown that, they can give a first-hand information on the failure before it takes place whereas in case of composites due to its brittle nature the failure takes place suddenly without any prior notification.
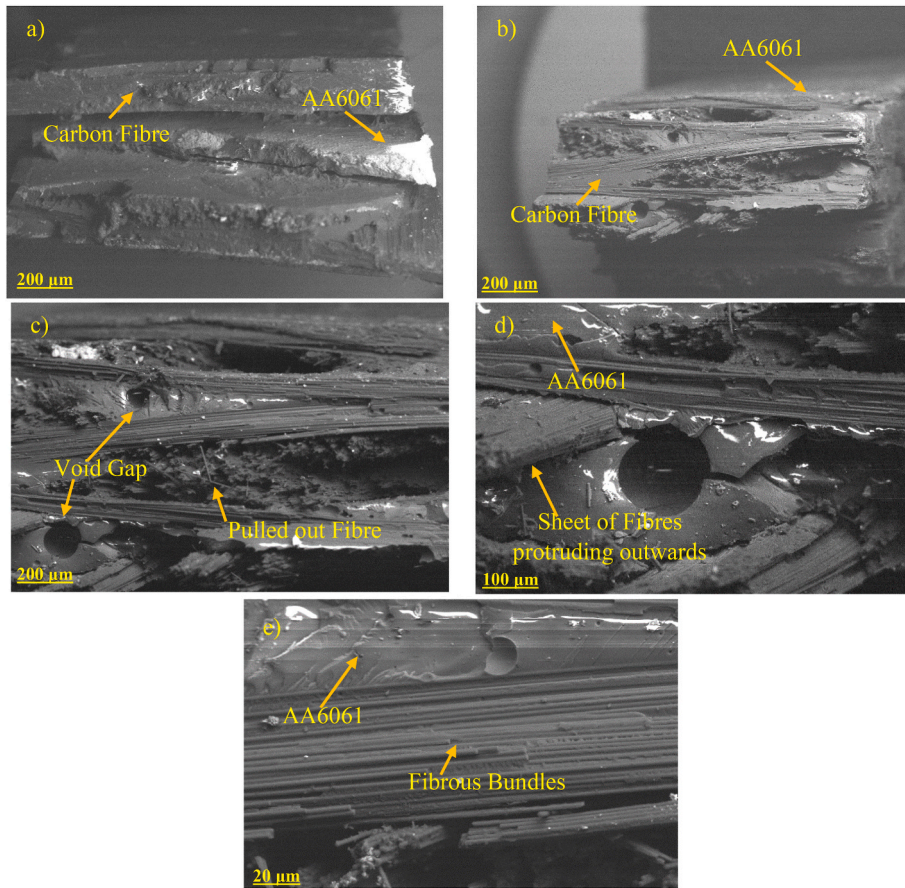
**Fig. 25.** Fractography of Fibre Metal Laminates at the failure zone at various magnifications: (**a**) cross sectional view, (**b**) magnified view, (**c**) damage mechanism, (**d**) magnified view of damaged mechanism, and (**e**) cross-sectional view of joined layers.
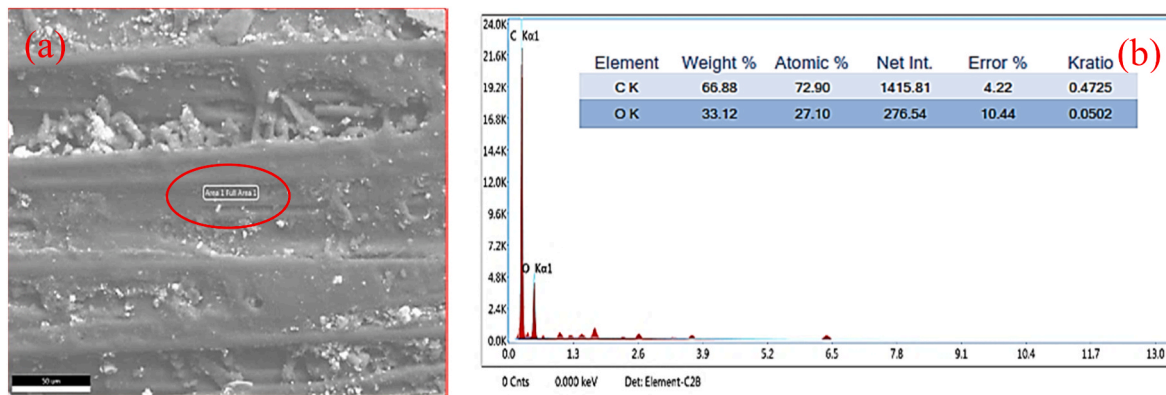


**Fig. 26.** (**a**) Area at which EDX image of Type – III specimen is taken, (**b**) EDX analysis of Type – III specimen.

- The mechanical properties were compared which showed that Type – I FML has an excellent property to be chosen as an aerospace material.
- Even though Type – II material also shows an improved result compared to Type – III material, still it does not prove to be a better replacement to Type – I as the values is in the mid between the two.
- Numerical simulation of the tensile and flexural tests helped to understand how the experimental trials behaves.
- The microstructural investigation showed the type of failure occurring in the three types of specimens and their nature. It helped to find out the orientation and bonding nature.

- EDX analysis showed the various elemental composition and showed that, there is a perfect bonding between the two types of materials namely carbon fibre and AA 6061 in FML.

The study evaluates the feasibility of alteration of stacking sequence to improve engineering properties of composites. The results could further be improved through improving the manufacturing process of hand lay-up process to vacuum bagging for controlling the layer thickness. In addition, there is need to investigate the interlaminar adhesion through anodization of metal for better strength.
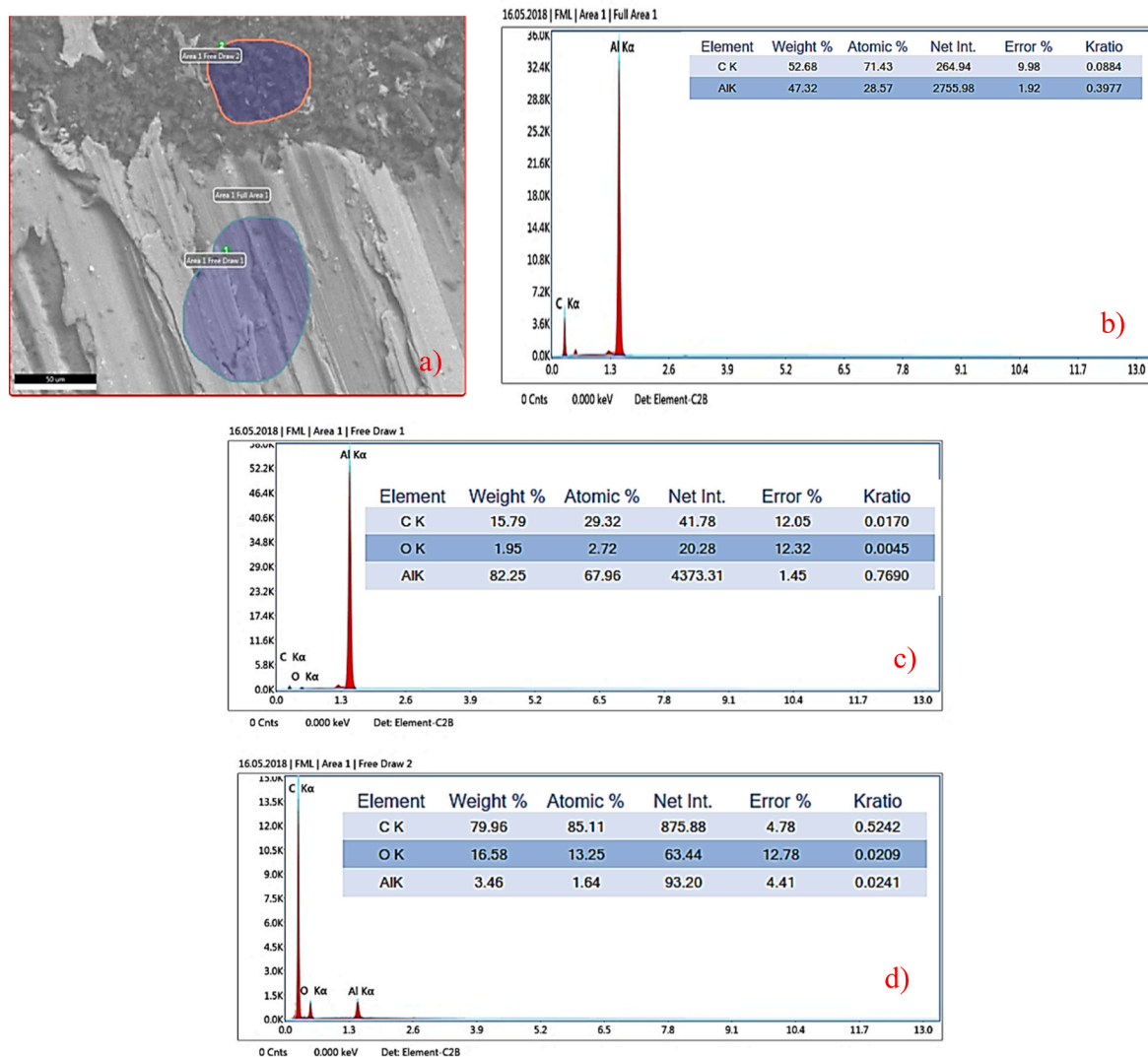
**Fig. 27.** (**a**) Areas at which EDX image of Type – I specimen has been taken, (**b**) EDX analysis at the central area, (**c**) EDX analysis at AA6061, (**d**) EDX analysis at carbon fibre.

## Author statement

I write on behalf of myself and all co-authors to confirm that the results reported in the manuscript are original and neither the entire work, nor any of its parts have been previously published. The authors confirm that the article has not been submitted to peer review, nor has been accepted for publishing in another journal. The author(s) confirms that the research in their work is original, and that all the data given in the article are real and authentic. If necessary, the article can be recalled, and errors corrected.

## Declaration of competing interest

The authors declare that they have no known competing financial interests or personal relationships that could have appeared to influence the work reported in this paper.

## References

[1] T. Sinmazçelik, E. Avcu, M.Ö. Bora, O. Çoban, A review: fibre metal laminates, background, bonding types and applied test methods, Mater. Des. 32 (2011) 3671–3685.

[2] N.A. Nassir, R.S. Birch, W.J. Cantwell, et al., The perforation resistance of aluminum-based thermoplastic FMLs, Appl. Compos. Mater. (2021) 1–19.

[3] Y. Yang, R. Boom, B. Irion, et al., Recycling of composite materials, Chem. Eng. Process: Process Intensificat. 51 (2012) 53–68.

[4] J. Bachmann, C. Hidalgo, S. Bricout, Environmental analysis of innovative sustainable composites with potential use in aviation sector—a life cycle assessment review, Sci. China Technol. Sci. 60 (2017) 1301–1317.

[5] E.C. Botelho, R.A. Silva, L.C. Pardini, M.C. Rezende, A review on the development and properties of continuous fiber/epoxy/aluminum hybrid composites for aircraft structures, Mater. Res. 9 (2006) 247–256.

[6] F. Pinto, L. Boccarusso, D. De Fazio, et al., Carbon/hemp bio-hybrid composites: effects of the stacking sequence on flexural, damping and impact properties, Compos. Struct. 242 (2020) 112148.

[7] W. Zhang, X. Ma, J. Lu, et al., Experimental characterization and numerical modeling of the interaction between carbon fiber composite prepregs during a preforming process, J. Manuf. Sci. Eng. 140 (2018).

[8] Polymer Composites in the Aerospace Industry, Elsevier, 2014.

[9] F.-L. Jin, S.-J. Park, Preparation and characterization of carbon fiber-reinforced thermosetting composites: a review, Carbon Lett. 16 (2015) 67–77.

[10] L. Che, Z. Zhou, G. Fang, et al., Cured shape prediction of fiber metal laminates considering interfacial interaction, Compos. Struct. 194 (2018) 564–574.

[11] J. Zhang, Y. Wang, G. Fang, et al., Application of energy dissipation approach for notched behavior in fiber metal laminates, Compos. Struct. 180 (2017) 809–820.

[12] L.M.G. Vieira, J.C. Dos Santos, T.H. Panzera, et al., Novel fibre metal laminate sandwich composite structure with sisal woven core, Ind. Crop. Prod. 99 (2017) 189–195.

[13] I. Mohammed, M.T.H. Sultan, M. Jawaid, et al., Mechanical properties of fibre-metal laminates made of natural/synthetic fibre composites, Bioresources 13 (2018) 2022–2034.

[14] A.A. Khurram, R. Hussain, H. Afzal, et al., Carbon nanotubes for enhanced interface of fiber metal laminate, Int. J. Adhesion Adhes. 86 (2018) 29–34.

[15] A.Z. Zakaria, K. Shelesh-nezhad, Introduction of nanoclay-modified fiber metal laminates, Eng. Fract. Mech. 186 (2017) 436–448.

[16] H. Aghamohammadi, S.N.H. Abbandanak, R. Eslami-Farsani, S.H. Siadati, Effects of various aluminum surface treatments on the basalt fiber metal laminates interlaminar adhesion, Int. J. Adhesion Adhes. 84 (2018) 184–193.

[17] M. Abouhamzeh, D. Nardi, R. Leonard, J. Sinke, Effect of prepreg gaps and overlaps on mechanical properties of fibre metal laminates, Compos. Appl. Sci. Manuf. 114 (2018) 258–268.

[18] G. Roebroeks, Fibre-metal laminates: recent developments and applications, Int. J. Fatig. 16 (1994) 33–42.

[19] S.H. Song, Y.S. Byun, T.W. Ku, et al., Experimental and numerical investigation on impact performance of carbon reinforced aluminum laminates, J. Mater. Sci. Technol. 26 (2010) 327–332.

[20] G.-C. Yu, L.-Z. Wu, L. Ma, J. Xiong, Low velocity impact of carbon fiber aluminum laminates, Compos. Struct. 119 (2015) 757–766.

[21] M.A. Azghan, R. Eslami-Farsani, The effects of stacking sequence and thermal cycling on the flexural properties of laminate composites of aluminium-epoxy/basalt-glass fibres, Mater. Res. Express 5 (2018), 025302.

[22] X. Zhou, Y. Zhao, X. Chen, et al., Fabrication and mechanical properties of novel CFRP/Mg alloy hybrid laminates with enhanced interface adhesion, Mater. Des. 197 (2021) 109251.

[23] G.D. Lawcock, L. Ye, Y.W. Mai, C.T. Sun, Effects of fibre/matrix adhesion on carbon-fibre-reinforced metal laminates—I.: residual strength, Compos. Sci. Technol. 57 (1998) 1609–1619.

[24] G.D. Lawcock, L. Ye, Y.W. Mai, C.T. Sun, Effects of fibre/matrix adhesion on carbon-fibre-reinforced metal laminates—II. impact behaviour, Compos. Sci. Technol. 57 (1998) 1621–1628.

[25] P. Cortes, W.J. Cantwell, The fracture properties of a fibre–metal laminate based on magnesium alloy, Compos. B Eng. 37 (2005) 163–170.

[26] B. Kolesnikov, L. Herbeck, A. Fink, CFRP/titanium hybrid material for improving composite bolted joints, Compos. Struct. 83 (2008) 368–380.

[27] J. Bieniaś, P. Jakubczak, B. Surowska, K. Dragan, Low-energy impact behaviour and damage characterization of carbon fibre reinforced polymer and aluminium hybrid laminates, Arch. Civ. Mech. Eng. 15 (2015) 925–932.

[28] G.R. Villanueva, W.J. Cantwell, The high velocity impact response of composite and FML-reinforced sandwich structures, Compos. Sci. Technol. 64 (2004) 35–54.

[29] M. Sadighi, R.C. Alderliesten, R. Benedictus, Impact resistance of fiber-metal laminates: a review, Int. J. Impact Eng. 49 (2012) 77–90.

[30] L.M. Vanani, H.M. Kashani, A.P. Anaraki, F.A. Ghasemi, Experimental and numerical investigation in failure of cracked aluminum plates repaired with bonded FML composite patch, under impact loading, Sci. Eng. Compos. Mater. 21 (2014) 493–503.

[31] A.M. Mukesh, N.R.J. Hynes, Mechanical properties and applications of fibre metal laminates, AIP Conf. Proc. 2142 (2019) 100002, https://doi.org/10.1063/1.5122456.

[32] G. Lawcock, L. Ye, Y.-W. Mai, C.-T. Sun, The effect of adhesive bonding between aluminum and composite prepreg on the mechanical properties of carbon-fiber-reinforced metal laminates, Compos. Sci. Technol. 57 (1997) 35–45.

[33] M. Ostapiuk, J. Bieniaś, Fracture analysis and shear strength of aluminum/CFRP and GFRP adhesive joint in fiber metal laminates, Materials 13 (2020) 7, https://doi.org/10.3390/ma13010007.

[34] N.G. Gonzalez-Canche, E.A. Flores-Johnson, J.G. Carrillo, Mechanical characterization of fiber metal laminate based on aramid fiber reinforced polypropylene, Compos. Struct. 172 (2017) 259–266.

[35] X. Zhang, Q. Ma, Y. Dai, et al., Effects of surface treatments and bonding types on the interfacial behavior of fiber metal laminate based on magnesium alloy, Appl. Surf. Sci. 427 (2018) 897–906.

[36] R. Santiago, W. Cantwell, M. Alves, Impact on thermoplastic fibre-metal laminates: experimental observations, Compos. Struct. 159 (2017) 800–817.

[37] J. Bieniaś, K. Dadej, B. Surowska, Interlaminar fracture toughness of glass and carbon reinforced multidirectional fiber metal laminates, Eng. Fract. Mech. 175 (2017) 127–145.